Materials Research. 2013; 16(3): 609-613
DOI: 10.1590/S1516-14392013005000028

A Nano-modified Superhydrophobic Membrane

***Antonio Ferreira Ávila*[a]*, *Aline Marques de Oliveira*[b], *Glenda Ribeiro de Barros Silveira Lacerda*[b], *Viviane Cristina Munhoz*[b], *Mayara Cele Gonçalves Santos*[b], *Patricia Figueiredo Santos*[b], *Matt Triplett*[c]**

[a]*Graduate Studies Program in Mechanical Engineering, Deparment of Mechanical Engineering, Universidade Federal de Minas Gerais – UFMG, Av. Antonio Carlos, 6627, CEP 31270-901, Belo Horizonte, MG, Brazil*
[b]*Chemistry Program, Centro Federal de Educação Tecnológica de Minas Gerais – CEFET-MG, Av. Amazonas, 5352, CEP 30421-169, Belo Horizonte, MG, Brazil*
[c]*Aviation and Missile Research Development and Engineering Center, AMSRD-AMR-WD-GA, Building 5420, Redstone Arsenal, 35898, USA*

Received: August 27, 2012; Revised: December 19, 2012

This paper focuses on the synthesis of super-hydrophobic membranes. The polymer used in this research is polystyrene (PS), which has low surface energy but not low enough to be characterized as a superhydrophobic material. As hydrophobicity is based on low energy surface and surface roughness, the electrospinning technique was selected as the manufacturing technique. N, N' dimethylformamide (DMF) was employed as the PS solvent. Two groups of PS/DMF solutions were investigated i.e. 20/80 and 35/65. To increase even more the hydrophobicity, nanoparticles of silica, graphene, cadmium, and zinc were dispersed into the PS/DMF solutions. In contrast to results previous published in literature, the PS/DMF weight ratio of 20/80 led to water contact angles (WCA) of 148°, which is higher than the contact angle for the 35/65 ratio, i.e. 143°. This fact seems to be due to the presence of non-evaporated solvent into the PS surface as the 35/65 solution was more viscous. The WCA for membranes with 0.5 wt. (%) of graphene reached 152°, 149°-153° for membranes with nanosilica addition, 151° with 5.0 wt. (%) CdS, and 153°, 163° and 168° with the addition of 5 wt. (%), 10 wt. (%) and 15 wt. (%) of ZnS, respectively.

Keywords: *nanomembranes, superhydrophobicity, graphene nanosheets, nanoparticles*

1. Introduction

As discussed by Du et al.[1], knowledge of interfacial water structures near hydrophobic surfaces is essential for understanding important surface problems involving water. The interaction between molecules of water and the surface can lead to self-cleaning surfaces. The idea of self-cleaning surfaces is not new. Nature has being producing these surfaces for centuries; the leaves of the lotus plant (Nelumbo nucifera) and wings of butterflies are some examples of natural self-cleaning surfaces. According to Lum et al.[2], the interest in self-cleaning surfaces is being motivated by possible industrial applications, e.g. solar energy panels including photovoltaics, exterior architectural glass, anti-freeze surfaces, and medical devices ranging from blood vessel replacement to wound management.

As argued by Zhai et al.[3], a superhydrophobic surface is able to repel water droplets completely; such surfaces exhibit water droplet advancing contact angles (CA) of 150° or higher. Likewise Lafuma and Quéré[4] pointed out that hydrophobicity and superhydrophobicity are related to the surface roughness since it brings as a consequence the increase on surface area, which leads to more loci for air-trapping. The two most relevant models that attempt to explain hydrophobicity are Cassie's and Wenzel's models. Cassie's model for hydrophobicity is based on the idea of water drops being settled over air bubbles, while the Wenzel's model associates hydrophobicity to surface roughness. However, none of them is capable of explaining hydrophobicity in its completeness. Miwa et al.[5] went further as they argued that surface roughness should be associated to surface energy in order to create a superhydrophobic behavior.

Several different approaches can be applied to artificially create hydrophobic and superhydrophobic surfaces. One option is to create micro texturized surfaces. This idea was tested by Lafuma and Quéré[4] with relative success. Although they were able to measure water CA of 164°, they realized that microtextures can be filled with water, especially when condensation is present. A similar approach was suggested by Lepore et al.[6], as they proposed surface modification of polystyrene plates by electrical discharge

*e-mail: aavila@netuno.lcc.ufmg.br

(corona treatment). Their results indicate that corona treatment is a helpful technique for tailoring surface tension of polymeric matrices. A different design was proposed by Jin et al[7]. They created a Gecko-like nanostructure based on a nano scale porous template which allows the formation of a heavily dense area of polystyrene nanotubes. Their results suggested the presence of a superhydrophobic surface behavior. Their water CA was around 162°. The major drawback of their work was its limitations due to the manufacturing complexity. A much simpler and easier process was proposed by Jiang et al.[8]. According to the authors, there are two requirements that must be fulfilled to obtain a superhydrophobic surface: surface roughness and low surface energy. Surface roughness can be acquired by deposition of nanofibers randomly oriented while low surface energy can be achieved by employing polystyrene (PS). The electrospinning technique was employed to obtain nanomembrane (random dispersion of nanofibers). The results presented by Jiang et al.[8] ranged from water contact angle from 139° to 162° depending on the matrix/solvent ratio. The best result reported by Jiang and colleagues was a mix of nanofibers and microspheres. The problem with this type of mixed structure is that it does not lead to a homogeneous dispersion which results in different water contact angles. Kang et al.[9] gave a step forward, using electrospinning and PS but with different operational parameters. Kang's matrix/solvent ratio reached 35% while Jiang's was limited to 25%.

This paper focuses on the development of hyper-hydrophobic micro/nano-membranes produced by electrospinning of PS/DMF solutions doped with nanoparticles. These membranes can be applied to glasses, windshields, or walls of surgery centers. Another important application of these membranes is on natural fibers and natural/green composites. Moisture absorption is a relevant issue for natural composites. Hyper-hydrophobic membranes can be applied to these natural composites as an "extra" protective layer to reset the barriers against moisture.

2. Material and Experimental Procedures

PS (Mw: 190,000 g.mol^{-1}), DMF (HPCL grade), ZnS and CdS were purchased from Sigma-Aldrich, nanosilica was supplied by Nissan Chemical, while the graphene was obtained using the procedure described in Ávila et al.[10]. The PS/DMF solutions were prepared under mild stirring (200 RPM) at a temperature of 40 °C. Once the PS solution reached the room temperature, particles were dispersed into the solution by ultra-sonication (at 20 kHz) for 30 minutes. The electrospinning technique described by Ko and Gandhi[11] and Ramakrishna et al.[12] was employed in this research. The electrospinning device is composed by different components, i.e. a high voltage supplier (Gamma High Voltage Research RR-30-150W, USA), a syringe pump (Harvard Apparatus, USA), a capillary tube with a stainless steel need (G18 blunted, diameter of 1.2 mm), and a collecting drum with a diameter of 100 mm.

To measure the water contact angle, an adjustable micropipette (0.1 μL-1.0 μL) was employed as the source of distillated water. The fibers/membranes morphology was investigated using a Quanta 200 - FEG - FEI – 2006 scanning electronic microscope. The public domain software for image-processing[13] was used for water contact angle measurements. The solution viscosity was measured using Cole-Parmer EW-98936 viscometer. Since there is no consensus on which polymer concentration can lead to the best results in terms of water CA (Jiang et al.[8] suggested 25 wt. (%), Kang et al.[9] employed 35 wt. (%)), this research selected the two extreme limits: 35 wt. (%) as upper bound and 20 wt. (%) as lower bound.

3. Results and Discussion

As commented by Kang et al.[9], PS is chemically hydrophobic. Carré[14] attributed this hydrophobicity to the PS low surface energy. His statement was based on Wenzel's model. However, the water CA is not enough to define PS as a superhydrophobic material. To enhance the "natural hydrophobicity" of PS surfaces, these surfaces have to be modified to increase their roughness. These changes can be made by dispersing nanoparticles into the electrospinning solution. Table 1 summarizes each set of experiments performed and their main parameters with respect to the electrospinning process. The electrical field density applied was kept constant and equal to 150 KV/m, i.e. 15 KV and distance needle tip to collector of 0.1 mm (100 mm), to all nine sets of experiments.

Table 1. Electrospinning parameters.

Group ID	PS [wt. (%)]	Nanosilica [wt. (%)]	Graphene [wt. (%)]	CdS [wt. (%)]	ZnS [wt. (%)]	Flow rate [μL/min]
1	20	---	---	---	---	33
2	35	---	---	---	---	33
3	20	---	0.5	--	---	17
4	20	0.5	---	---	---	17
5	20	1.0	---	---	---	17
6	20	---	---	5	---	17
7	20	---	---	---	5	17
8	20	---	---	---	10	17
9	20	---	---	---	15	17

Figure 1 shows the dynamic viscosity for each set of experiments. As it can be noticed, as rotation increases (high shear rates), the dynamic viscosity decreases. However, as discussed by Guerrini et al.[15], during the electrospinning process small shear rates are developed because of the small flow rate. To keep the same electrostatic forces in all cases, the flow rate for group #2 had to be increased since this group had a higher dynamic viscosity. This happens because group 2 has a 35 wt. (%) of PS. The same flow rate was used in group #1 for comparison purposes. In groups #3 through #9, the small variation on dynamic viscosity can be attributed to the presence of nanoparticles dispersion.

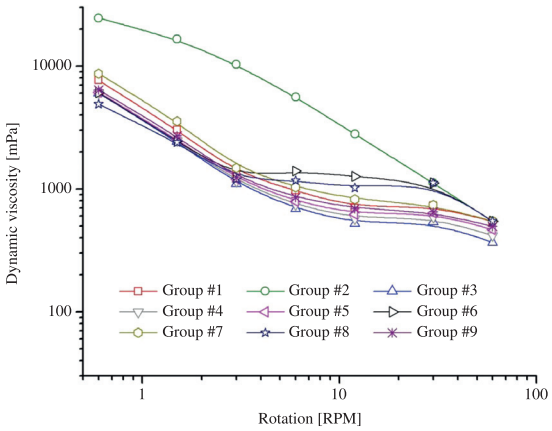

Figure 1. Dynamic Viscosity. Group #1: 20 wt. (%) PS and no nanoparticle; group #2: 35 wt. (%) PS and no nanoparticle; group #3: 20 wt. (%) PS and 0.5 wt. (%) graphene; group #4: 20 wt. (%) PS and 0.5 wt. (%) nanosilica; group #5: 20 wt. (%) PS and 1 wt. (%) nanosilica; group #6: 20 wt. (%) PS and 5 wt. (%) CdS; group #7: 20 wt. (%) PS and 5 wt. (%) ZnS; group #8: 20 wt. (%) PS and 10 wt. (%) ZnS; group #9: 20 wt. (%) PS and 15 wt. (%) ZnS.

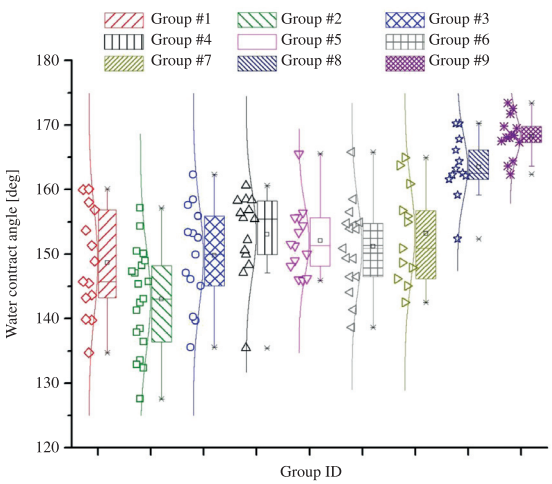

Figure 2. Water Contact Angle. Group #1: 20 wt. (%) PS and no nanoparticle; group #2: 35 wt. (%) PS and no nanoparticle; group #3: 20 wt. (%) PS and 0.5 wt. (%) graphene; group #4: 20 wt. (%) PS and 0.5 wt. (%) nanosilica; group #5: 20 wt. (%) PS and 1 wt. (%) nanosilica; group #6: 20 wt. (%) PS and 5 wt. (%) CdS; group #7: 20 wt. (%) PS and 5 wt. (%) ZnS; group #8: 20 wt. (%) PS and 10 wt. (%) ZnS; group #9: 20 wt. (%) PS and 15 wt. (%) ZnS.

A summary of all water CA is shown in Figure 2. The statistical analysis (Levene's test) indicates that the nine sets are significantly different for a critical p-value of 0.05. The large variations on water CA measurements can be attributed to the random distribution of fibers that creates a very rough surface. As the hydrophobicity increases, the interface between the beginning of the water droplet and the end of the surfaces becomes more defined and the standard deviation on water CA measurements decreases. As it can be noticed, group #1 presented a higher water CA (147.96° ± 8.51°) than group #2 (143.01° ± 7.88°). This can be explained by the increase on viscosity, as shown in Figure 1. According to Ko and Gandhi[11] less viscous solutions lead to smaller fiber diameters. Furthermore, as discussed by Carré[14], smaller fiber diameters increase the surface roughness and consequently the water contact angle.

The addition of nanoparticles created the conditions for larger water CA in all cases, when compared against the two sets of experiments (groups #1 and #2) without nanoparticles. In group #3, the addition of graphene led to an increase on water CA (152.09° ± 5.35°). A high resolution scanning electron microscopy (HRSEM) analysis (Figure 3a) reveals a rough surface with discontinuous groove marks of 120 ± 5 nm in length and 7 ± 0.8 nm in width. The roughness associated to the PS low surface tension could explain the increase on water CA. Although the results can suggest that an increase on graphene concentration can generate even better values of water CA, there is a drawback for using graphene. As the graphene density is too low (<0.5 g.cm^{-3} in the "powder" form), if we increase the graphene weight percentage, we likely produce a much higher viscous solution. For practical purposes, the 0.5 wt. (%) seems to be the graphene upper bound for 20/80 PS/DMF solutions.

The water CA values for Groups #4 (149.79° ± 7.85°) and #5 (153.09° ± 6.58°) are on superhydrophobic range. Nonetheless, there is no linear relationship between the nanosilica content and the water CA. This non-linearity can be explained by differences in the fibers morphology. By observing Figures 3b, c, it is possible to notice a large increase in porosity for the 1.0 wt. (%) nanosilica. The increase in porosity leads to changes in fiber diameters and shapes. Unfortunately, these changes are uncontrollable and therefore unacceptable for industrial applications.

Groups #6 through #9 reveals a nonlinear increase on water CA. The addition of cadmium nanoparticles led to a water CA of 151.22° ± 6.80°, while the Zn addition produced conditions to water CA of 153.20° ± 7.47°, 163.49° ± 4.93°, and 168.22° ± 3.19° for 5 wt. (%), 10 wt. (%) and 15 wt. (%), respectively. The increases on water CA can be attributed to the presence of nanoparticles on the fibers' surface (See Figures 3d through 3g). The differences on Cd and Zn sizes (284.39 ± 8.71 nm and 323.34 ± 6.98 nm) and their distribution could be the reason for the differences in WCA. Although cadmium fibers could be classified as superhydrophobic, environmental issues are a serious concern. The additional increase on water CA on Groups #8 and #9 could be explained by the agglomeration of Zn

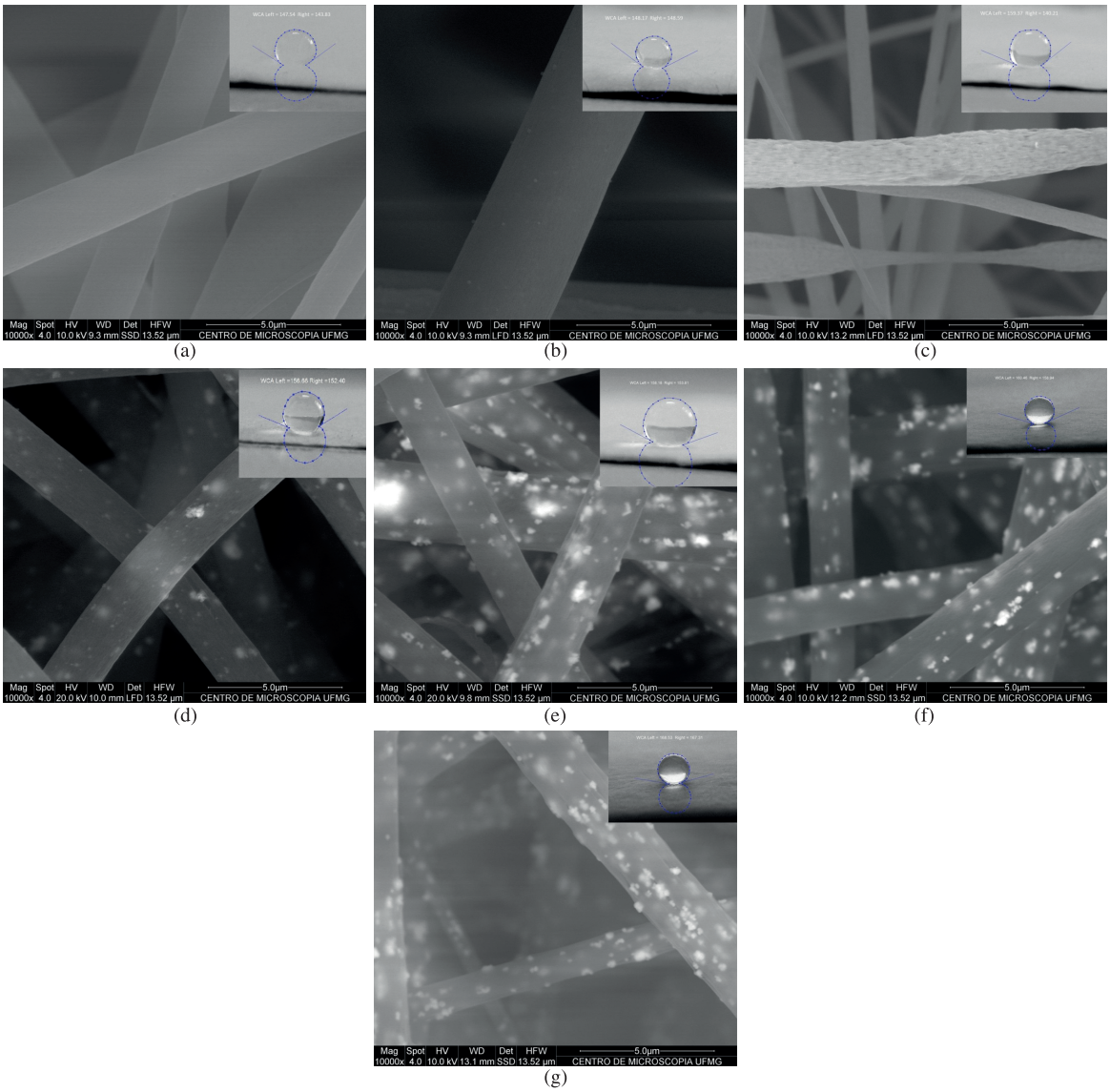

Figure 3. HRSEM images of electrospun fibers from PS/DMF solutions. (a) 0.5 wt. (%) graphene; (b) 0.5 wt. (%) of nanosilica; (c) 1 wt. (%) of nanosilica; (d) 5 wt. (%) Cd; (e) 5 wt. (%) Zn; (f) 10 wt. (%) Zn; (g) 15 wt. (%) Zn.

nanoparticles on the fibers' walls. These agglomerations are on the order of 378.92 ± 8.78 nm and 561.31 ± 11.94 nm, for the 10 wt. (%) and 15 wt. (%), respectively. With the increase of nanoparticles "clusters", roughness is enhanced which leads to a higher water contact angle. Finally, given the water CA values obtained, it is possible to categorize Group #9 (addition of 15 wt. (%) of ZnS) as a hyper-hydrophobic membrane.

4. Conclusions

PS fibers doped with nanoparticles were prepared by electrospinning. In contrast to results previous published in literature, the PS/DMF weight ratio of 35/65 did not lead to higher water contact angles. This fact can be attributed to the presence of non-evaporated solvent into the PS surface. Contrary to results previous published in literature, the PS/DMF weight ratio of 20/80 lead to water contact angles (WCA) of 148°, which is higher than the one obtained for the 35/65 ratio, i.e. 143°. The WCA for membranes with 0.5 wt. (%) of graphene reached 152°, 149°-153° with the addition of nanosilica, 151° with 5.0 wt. (%) CdS, and 153°, 163° and 168° with the addition of 5 wt. (%), 10 wt. (%) and 15 wt. (%) of ZnS, respectively. The fiber morphology was also affected by the addition of nanoparticles. Continuous axial groove marks were formed with the addition of graphene, while the addition of nanosilica around 1.0 wt. (%) generated non-homogeneous fibers regardless of the cross section and porosity. The addition of Cd and Zn nanoparticles generated "nano-clusters" on fibers' surface, which altered the overall roughness and consequently the WCA.

Acknowledgments

This research was supported in part by the AFOSR under contract FA9550-10-1-0050, the Brazilian Research Council (CNPq) under grants number 303447/2011-7, 472583/2011-5 and the Minas Gerais State Research Foundation (FAPEMIG) grant TEC-PPM00192-12. The authors are grateful to the UFMG's Center of Microscopy and Microanalysis for the technical support.

References

1. Du Q, Freysz E and Shen YR. Surface Vibrational Spectroscopic Studies of Hydrogen Bonding and Hydrophobicity. *Science*. 1994; 264(21):826-828. http://dx.doi.org/10.1126/science.264.5160.826
2. Lum K, Chandler D and Weeks JD. Hydrophobicity at Small and Large Length Scales. *Journal of Physical and Chemistry B*. 1999; 103(12):4570-4577. http://dx.doi.org/10.1021/jp984327m
3. Zhai L, Cebeci FC, Cohen RE and Rubner MF. Stable Superhydrophobic Coatings from Polyelectrolyte Multilayers. *Nano Letters*. 2004; 4(7):1349-1353. http://dx.doi.org/10.1021/nl049463j
4. Lafuma A and Quéré D. To read this story in full you will need to login or make a payment (see right). *Nature Materials*. 2003; 2(7):457-460. http://dx.doi.org/10.1038/nmat924
5. Miwa M, Nakajima A, Fujishima A, Hashimoto K and Watanabe T. Effects of the Surface Roughness on Sliding Angles of Water Droplets on Superhydrophobic Surfaces. *Langmuir*. 2000; 16(10):5754-5760. http://dx.doi.org/10.1021/la991660o
6. Lepore E, Faraldi P, Bongini D, Boarino L and Pugno N. Plasma and thermoforming treatments to tune the bio-inspired wettability of polystyrene. *Composites Part B*. 2012; 43(2):681-690. http://dx.doi.org/10.1016/j.compositesb.2011.05.028
7. Jin M, Feng X, Feng L, Sun T, Zhai J, Li T et al. Superhydrophobic Aligned Polystyrene Nanotube Films with High Adhesive Force. *Advanced Materials*. 2005; 17(6):1977-1981. http://dx.doi.org/10.1002/adma.200401726
8. Jiang L, Zhao Y and Zhai J. A Lotus-Leaf-like Superhydrophobic Surface: A Porous Microsphere/Nanofiber Composite Film Prepared by Electrohydrodynamics. *Angewandte Chemie*. 2004; 116(15):4438-4441. http://dx.doi.org/10.1002/ange.200460333
9. Kang M, Jung R, Kim H-S and Jin H-J. Preparation of superhydrophobic polystyrene membranes by electrospinning. *Colloids and Surfaces A*: Physicochemical and Engineering Aspects. 2008; 313-314(2):411-414. http://dx.doi.org/10.1016/j.colsurfa.2007.04.122
10. Ávila AF, Yoshida MI, Carvalho MGR, Dias EC and De Ávila Junior J. An investigation on post-fire behavior of hybrid nanocomposites under bending loads. *Composites Part B*. 2010; 41(2):380-387. http://dx.doi.org/10.1016/j.compositesb.2010.02.002
11. Ko FK and Gandhi MR. Producing Nanofiber Structures by Electrospinning for Tissue Engineering. In: Brown PJ and Stevens K, editors. *Nanofibers and Nanotechnology in Textiles.* Woodhead Publishing; 2007. p. 22-44. http://dx.doi.org/10.1533/9781845693732.1.22
12. Ramakrishna S, Fujiaha K, Teo W-E, Lim T-C and Ma Z. *Introduction to Electrospinning and Nanofibers*. New York: World Scientific; 2005. p. 90-154. http://dx.doi.org/10.1142/9789812567611_0003
13. Collins TJ. ImageJ for microscopy. *BioTechniques*. 2007; 43(1):S25-S30. http://dx.doi.org/10.2144/000112517
14. Carré A. Polar interactions at liquid/polymer interfaces. *Journal of Adhesion Science and Technology*. 2007; 21(10):961-981. http://dx.doi.org/10.1163/156856107781393875
15. Guerrini LM, Branciforti MC, Canova T and Bretas RES. Electrospinning and characterization of polyamide 66 nanofibers with different molecular weights. *Materials Research.* 2009; 12(2):181-190. http://dx.doi.org/10.1590/S1516-14392009000200012